Nature Environment and Pollution Technology
An International Quarterly Scientific Journal

p-ISSN: 0972-6268
(Print copies up to 2016)
e-ISSN: 2395-3454

Vol. 25 | No. 1 | Article ID D1792 | 2026

Original Research Paper

https://doi.org/10.46488/NEPT.2026.v25i01.D1792

Open Access Journal

Biocells for Waste Valorization: Enhancing Methane Production and Leachate Management in the Anaerobic Degradation of Green Waste and WWTP Biosolids from Ambato, Ecuador

Rodny Peñafiel[1], Nelly Esther Flores Tapia[1], Celia Margarita Mayacela Rojas[2], Freddy Roberto Lema Chicaiza[3], Doménica Belén Guamán Canseco[1] and Marlon Fabricio Muñoz Arroba[1]

[1]Environmental Laboratory, Faculty of Food Science and Biotechnology Engineering, Technical University of Ambato, Ecuador
[2]Faculty of Civil and Mechanical Engineering, Research and Development Directorate, Technical University of Ambato, Ecuador
[3]Industrial Engineering Program, Faculty of Systems, Electronics and Industrial Engineering, Technical University of Ambato, Ecuador
†Corresponding author: Rodny Peñafiel; rd.penafiel@uta.edu.ec

Abbreviation: Nat. Env. & Poll. Technol.
Website: www.neptjournal.com

Received: 27-02-2025
Revised: 25-05-2025
Accepted: 27-05-2025

Key Words:

Bioreactor landfills
Biocells
Methane generation
Leachate recirculation
Wastewater treatment
Biosolids
Heavy metals
Solid waste management
Environmental biotechnology

Citation for the Paper:

Peñafiel, R., Flores Tapia, N. E., Mayacela Rojas, C. M., Lema Chicaiza, F. R., Guamán Canseco, D. B., and Muñoz Arroba, M. F., 2026. Biocells for waste valorization: enhancing methane production and leachate management in the anaerobic degradation of green waste and WWTP biosolids from Ambato, Ecuador. *Nature Environment and Pollution Technology*, 25(1), D1792. https://doi.org/10.46488/NEPT.2026.v25i01.D1792

Note: From 2025, the journal has adopted the use of Article IDs in citations instead of traditional consecutive page numbers. Each article is now given individual page ranges starting from page 1.

ABSTRACT

The disposal of solid waste in conventional landfills poses critical environmental challenges, including uncontrolled greenhouse gas emissions and highly contaminated leachate. Bioreactor landfills with leachate recirculation offer an effective alternative, accelerating organic matter degradation and enhancing methane production for energy recovery. The present study investigates methane generation, leachate characteristics, and the stabilization of organic matter in laboratory-scale biocells that incorporate biosolids from the Ambato Wastewater Treatment Plant (WWTP), along with compost and green waste. Three replicate biocells were operated over 12 weeks with leachate recirculation to optimize nutrient removal and biogas production. Methane generation stabilized after 21 days, while phosphorus and ammonium concentrations in the leachate ranged from 10-15 $mg.L^{-1}$ and 50-80 $mg.L^{-1}$, respectively. Heavy metal concentrations significantly decreased, with final cadmium and chromium levels falling below regulatory discharge limits, reaching 0.02 $mg.L^{-1}$ and 0.05 $mg.L^{-1}$, respectively. Chemical Oxygen Demand (COD) was reduced by 85%, reaching a final concentration of approximately 300 $mg.L^{-1}$. These findings highlight the feasibility of incorporating WWTP biosolids in biocells to enhance organic solid waste degradation, sustainable landfill leachate management, and renewable energy generation in Ambato, Ecuador.

INTRODUCTION

Municipal landfills remain the predominant method for disposing of urban solid waste in developing countries due to their operational simplicity and high capacity for managing residual materials (Zhang et al. 2019). This is the case of Ambato, an Andean city in Ecuador with nearly 190,000 inhabitants and an estimated solid waste generation of approximately 300 tons per day (GAD Municipal de Ambato 2016, Instituto Nacional de Estadística y Censos (INEC) 2023). However, global solid waste generation has increased significantly-from 635 million tons in 1965 to 1,999 million tons in 2015-and is projected to reach 3,539 million tons by 2050 (Chen et al. 2020). The continued accumulation of solid waste in landfills poses serious environmental challenges, particularly concerning the generation of landfill gas (LFG) and leachate.

Waste decomposition in landfills primarily occurs through anaerobic microbial processes. These processes are facilitated by bacteria such as *Sporanaerobacter acetigenes*, *Clostridium sporogenes*, *Methanomicrobiales* and *Methanosarcinales*, which contribute to the production of gaseous compounds (Shao et al. 2021, Yang et al. 2021). The resulting LFG typically consists of CH_4 (50–60%), CO_2 (40–50%), and volatile organic compounds (VOCs). In many cases, it is either directly released

into the atmosphere or flared without adequate quality controls, exacerbating air pollution and posing risks to human health (Werkneh 2022). Methane emissions from landfills are of particular concern, given that CH_4 has a global warming potential (GWP) 28–36 times greater than CO_2 over 100 years (IPCC 2023). Landfills account for approximately 5% of global greenhouse gas emissions, contributing significantly to climate change (EPA 2024).

The disposal of household and industrial solid waste in landfills introduces various hazardous compounds that are difficult to biodegrade, including organic solvents, pesticides, herbicides, BTEX compounds (benzene, toluene, ethylbenzene, and xylene), and heavy metals such as cadmium (Cd) and hexavalent chromium (Cr^{6+}) (Essien et al. 2022, Kjeldsen et al. 2002, Vaverková 2019). Leachate can act as a transport medium for these pollutants, leading to surface and groundwater contamination and frequently migrating into surrounding soils through percolation (Hadi 2023). Leached contaminants, including Cd^{2+}, Pb^{2+}, Zn^{2+}, and Cu^{2+}, are highly toxic, carcinogenic, and resistant to degradation (Hussein et al. 2021). Furthermore, toxicological studies indicate that certain leachates exhibit mutagenic properties, reinforcing the need for effective leachate management strategies (Vaverková 2019). These strategies involve the use of enhanced landfill cover materials (Sanoop et al. 2024), leachate collection and recirculation, as well as advanced treatment processes, including biological, physicochemical, and oxidative techniques (Mojiri et al. 2021).

Despite the availability of advanced biogas management and leachate treatment technologies, their implementation is often hindered in developing countries due to financial constraints and infrastructure limitations. Consequently, methane emissions remain largely uncontrolled, and leachate frequently contaminates surrounding soil and water sources due to inadequate treatment systems (Zhang et al. 2024).

Biocells offer a promising alternative to conventional landfills, as they incorporate leachate recirculation strategies that enhance microbial activity, accelerate organic matter degradation, and promote rapid waste stabilization. This approach optimizes conditions for methane production while simultaneously improving the reduction of Chemical Oxygen Demand (COD) in leachate compared to traditional landfill treatment methods (Budihardjo et al. 2021). Leachate recirculation not only enhances bacterial metabolic activity but also facilitates more efficient biodegradation by supplying essential nutrients and microorganisms. Consequently, biocells improve waste decomposition, reclaim landfill airspace, and increase CH_4 production efficiency, which can be harnessed as a renewable energy source. Unlike conventional landfills, where biogas is often released into the environment with harmful consequences, biocells provide a controlled degradation environment that maximizes methane recovery (Japperi et al. 2021).

The primary objective of this study is to evaluate methane production and characterize the leachate generated by laboratory-scale biocells used for solid waste disposal, incorporating biosolids from the Ambato Wastewater Treatment Plant (WWTP) and green waste from local markets in Ambato. The research focuses on implementing a solid-phase biodigestion system to decompose organic matter, operating biocells over a stabilization period of 12 weeks, and assessing performance through biogas quantification, leachate characterization, and solid-phase analysis.

Integrating WWTP biosolids with green waste and intermediate compost layers in a biocell system presents challenges, particularly due to the presence of recalcitrant organic contaminants and heavy metals, which may complicate leachate management (Kjeldsen et al. 2002). Additionally, certain residues within biosolids can slow biodegradation, potentially extending the stabilization period. This study aims to address these concerns and evaluate the feasibility of biocell technology as an alternative waste management approach for Ambato. A successful implementation could reduce landfill inputs, mitigate environmental impacts, promote methane as a renewable energy source, and improve overall waste stabilization (Kumar et al. 2011).

MATERIALS AND METHODS

Biocell Design and Operation

The biocell was designed to minimize compaction within the waste mass to ensure uniform moisture distribution and adequate hydraulic conductivity, thereby preventing clogging (Aldrawsha et al. 2020). The biocells were constructed within cylindrical columns, incorporating alternating layers of compost, green waste, and WWTP biosolids (see Fig. 1). A sand-gravel layer at the base facilitated drainage, while an additional sand layer at the top ensured uniform leachate distribution. Compost was obtained from agricultural supply centers. The organic waste materials consisted of rabbit manure compost, while green waste comprised lettuce and cabbage residues. Organic waste was collected from markets in Ambato and transported to the laboratory in plastic bags. Dehydrated biosolid samples were collected from the output of the

Table 1: Weight Distribution of Layered Materials for Biocell Assembly.

Layered Material	Biocell1	Biocell 2	Biocell 3
Sand, [g]	4215	4004	3816
Compost [g]	397	363	436
Green waste [g]	311	296	270
WWTP Biosolids [g]	783	722	792
Compost [g]	422	332	497
Green waste [g]	294	290	277
WWTP biosolids [g]	758	713	746
Compost [g]	477	371	623
Sand [g]	1559	2215	1772

biosolids centrifuge at the Ambato Wastewater Treatment Plant (WWTP). To prevent decomposition prior to the incorporation of organic material into the biocell, samples were stored under refrigeration at 4°C, following the protocols established in Standard Method 1060: Collection and Preservation of Samples (APHA 2017). Table 1 presents the weights of the different material layers incorporated into the biocells.

The leachate produced by the biocell was recirculated to maintain a uniform moisture distribution throughout the waste mass, with cycles occurring approximately every two hours, driven by peristaltic pumps operating at a flow rate of 4.2 mL.min^{-1}. This interval was adjusted as needed based on the permeability and moisture retention capacity of the waste materials.

Leachate and biogas generation were systematically monitored weekly to evaluate the progression of the biodegradation process.

Leachate Sampling and Characterization

Leachate samples were collected weekly to monitor chemical changes within the biocells. All analyses were conducted in accordance with the Standard Methods for the Examination of Water and Wastewater (APHA 2017). All chemical analyses were performed in triplicate, and standard deviation coefficients were calculated. Conductivity and pH measurements were taken using a HANNA HI839800 multiparametric meter. Chemical analyses for sulfate, phosphate, iron, magnesium, ammonium, chemical oxygen demand (COD), sulfide, and hexavalent chromium concentrations were conducted using photometric methods with the HI83399 Hanna photometer. For heavy metal analysis, including total chromium and cadmium, Graphite Furnace Atomic Absorption Spectrometry (GFAAS) was conducted using the PG Instruments AA500 spectrometer.

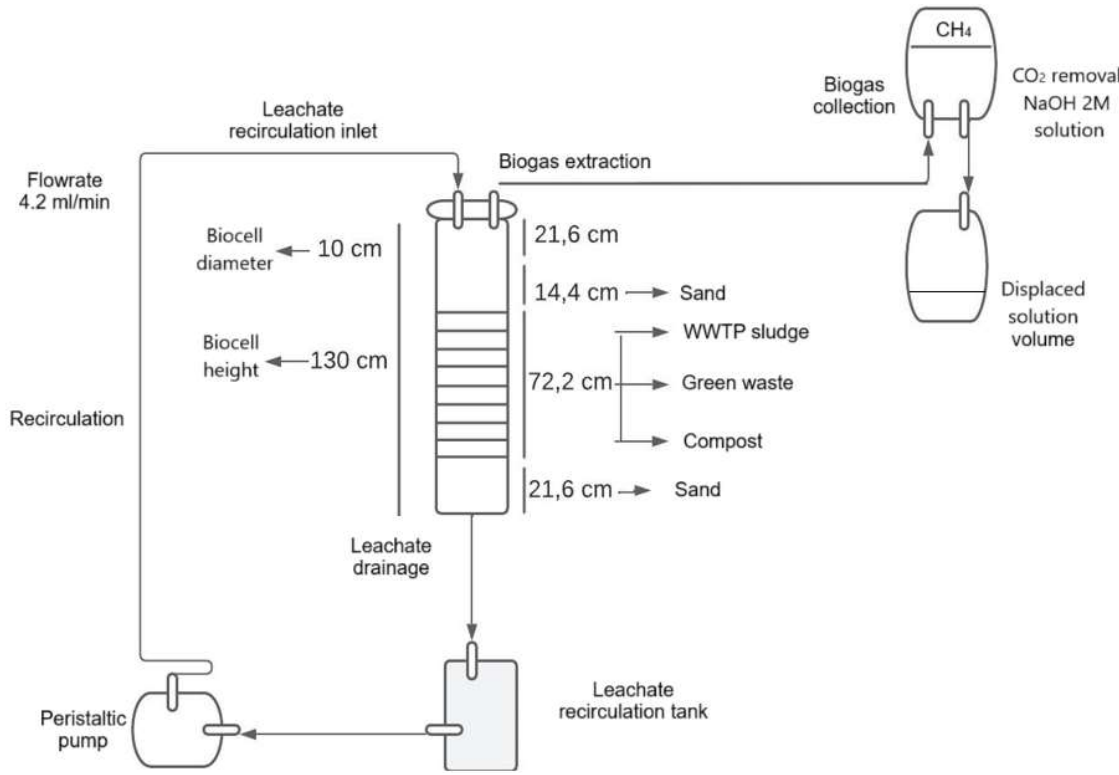

Fig. 1: Schematic of the Biocell Design for Organic Matter Decomposition.

Calibration curves with Pearson correlation coefficients ($R^2 > 0.98$) were applied.

Characterization of Waste Components (Compost, Biosolids, and Organic Matter)

The moisture content of the organic waste was determined by drying samples at 105°C for 24 h in a BINDER ED-400 oven following the methodology of 2540 D. Volatile solids were measured by igniting the dried samples at 550°C for two h in a muffle furnace, Biobase MC10-12, using the standard method SM 2540 G (APHA 2017). The biosolids samples were subjected to acid digestion to extract analytes present in the WWTP biosolids, following the EPA 3051A method (EPA 2007). Photometric methods using the HANNA HI83399 multiparameter photometer were employed to determine total phosphorus, potassium, magnesium, calcium, sulfate, manganese, iron, aluminum, copper, molybdenum, and zinc in solubilized dry biosolids. The concentrations of arsenic, cadmium, chromium, nickel, and lead in digested biosolids samples were determined by Graphite Furnace Atomic Absorption Spectrometry (GFAAS) using a PG-500 Atomic Absorption Spectrophotometer. Mono-elemental standards (AccuStandard, 1000 $\mu g.L^{-1}$) were used for calibration.

Biogas Collection and Methane Gas Quantification

Biogas was collected using a volumetric method, which consisted of a closed system with two 1-liter amber glass bottles and a 2M NaOH solution. One bottle contained the NaOH solution to capture CO_2, allowing for the collection of purified methane as biogas (Fig. 2). This setup enabled the quantification of methane output by utilizing an amber glass bottle containing a 2M NaOH solution, connected to an adjacent empty container through a tube. As biogas exerted pressure, it displaced the NaOH solution from one bottle to the other, effectively absorbing CO_2 from the biogas. The methane content was then determined by measuring the weight of the displaced NaOH solution (Nopharatana et al. 1998, Sorensen & Ahring 1993).

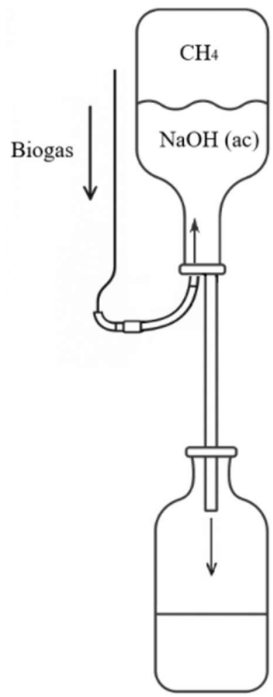

Fig. 2: Schematic of CH_4 Collection System Using NaOH Absorption.

Materials and Chemicals

All reagents were of analytical grade: NH_4Cl and $C_2H_3NaO_2$ (Sigma-Aldrich), KH_2PO_4 and H_3BO_3 (Merck). Magnesium chloride hexahydrate ($MgCl_2 \cdot 6H_2O$, 82.4 $mg.L^{-1}$), calcium chloride ($CaCl_2$, 10 $mg.L^{-1}$), sodium bicarbonate ($NaHCO_3$, 3000 $mg.L^{-1}$), and zinc chloride ($ZnCl_2$, 0.1 $mg.L^{-1}$) were supplied by Thermo Fisher Scientific. Yeast extract (10 $mg.L^{-1}$) was purchased from Becton, Dickinson, and Company (BD). Trace elements included ferrous chloride tetrahydrate ($FeCl_2 \cdot 4H_2O$, 2 $mg.L^{-1}$) and manganese chloride ($MnCl_2$, 0.1 $mg.L^{-1}$) from Sigma-Aldrich, ammonium molybdate tetrahydrate ($(NH_4)_6Mo_7O_{24} \cdot 4H_2O$, 0.1 $mg.L^{-1}$), cobalt chloride hexahydrate ($CoCl_2 \cdot 6H_2O$, 2 $mg.L^{-1}$), and aluminum sulfate hydrate ($Al_2(SO_4)_3 \cdot 18H_2O$, 0.1 $mg.L^{-1}$) from Merck, nickel nitrate hexahydrate ($Ni(NO_3)_2 \cdot 6H_2O$, 0.1 $mg.L^{-1}$), copper sulfate pentahydrate ($CuSO_4 \cdot 5H_2O$, 0.1 $mg.L^{-1}$), and sodium selenite pentahydrate ($Na_2SeO_3 \cdot 5H_2O$, 0.1 $mg.L^{-1}$) from Sigma-Aldrich. EDTA (1 $mg.L^{-1}$) was also obtained from Sigma-Aldrich. The pH was adjusted using hydrochloric acid (HCl, 0.001 $mg.L^{-1}$) from Merck.

Preparation of Basal Medium

The basal medium contained 280 $mg.L^{-1}$ of ammonium chloride (NH_4Cl), 250 $mg.L^{-1}$ of monopotassium phosphate (KH_2PO_4), 82.4 $mg.L^{-1}$ of magnesium chloride hexahydrate ($MgCl_2 \cdot 6H_2O$), 10 $mg.L^{-1}$ of calcium chloride ($CaCl_2$), 3000 $mg.L^{-1}$ of sodium bicarbonate ($NaHCO_3$), and 10 $mg.L^{-1}$ of yeast extract. To promote the methanogenic activity of microorganisms, 3204.5 $mg.L^{-1}$ of anhydrous sodium acetate ($C_2H_3NaO_2$) was added. The pH of the basal medium was adjusted to a range of 7.1 to 7.3 and measured using an OAKTON N16M3F pH meter.

Trace elements and micronutrients were also incorporated, including 0.1 $mg.L^{-1}$ of boric acid (H_3BO_3), zinc chloride ($ZnCl_2$), manganese chloride ($MnCl_2$), ammonium molybdate tetrahydrate ($(NH_4)_6Mo_7O_{24} \cdot 4H_2O$), aluminum sulfate hydrate ($Al_2(SO_4)_3 \cdot 18H_2O$), nickel nitrate

hexahydrate ($Ni(NO_3)_2 \cdot 6H_2O$), copper sulfate pentahydrate ($CuSO_4 \cdot 5H_2O$), and sodium selenite pentahydrate ($Na_2SeO_3 \cdot 5H_2O$). The medium also contained 2 $mg.L^{-1}$ of ferrous chloride tetrahydrate ($FeCl_2 \cdot 4H_2O$) and cobalt chloride hexahydrate ($CoCl_2 \cdot 6H_2O$). Additionally, 1 $mg.L^{-1}$ of EDTA and 0.001 $mg.L^{-1}$ of hydrochloric acid (HCl) were included to enhance nutrient stability and bioavailability.

Statistical Analysis

Repeated measures ANOVA was applied to assess whether statistically significant changes occurred over the 12 weeks within each biocell for all monitored parameters. This analysis was performed using the AnovaRM function from Python's *statsmodels* library (v0.14.0), following a within-subjects design based on weekly triplicate measurements, which allowed for the evaluation of temporal trends. In parallel, a one-way ANOVA was performed using the f_oneway function from Python's *scipy*. *Stats* module to determine whether the mean values differed significantly among the three biocells.

RESULTS AND DISCUSSION

Characteristics of Waste Components: Compost, WWTP Biosolids, and Organic Matter

The biocells were designed to accelerate the decomposition of solid waste and enhance biogas production through recirculation. Organic matter plays a key role in this process by serving as the primary substrate for anaerobic digestion. Table 2 summarises the physicochemical characteristics of the three organic substrates used in the biocell system, i.e., WWTP biosolids, compost, and green waste. The table presents their pH, moisture content (wet basis), percentage of volatile solids, and the total nitrogen and phosphorus content (dry basis). These parameters help assess the suitability and biodegradability of each substrate within the anaerobic environment.

As shown in the data, compost has a slightly basic pH of 8.6 ± 0.5, indicating a natural buffering capacity that can support pH stability within the system and potentially enhance methanogenic activity. In contrast, WWTP biosolids (7.7 ± 0.1) and green waste (7.2 ± 0.1) provide a more neutral environment, supporting microbial stability but potentially becoming susceptible to acidification under high organic loads. Moisture content is an important factor influencing hydrolysis efficiency, and in this study, green waste showed a moisture level of 80.6%. This value is slightly lower than those reported in the literature, which range from 90% to 94.7% (Sanchez-Salvador et al. 2022). In contrast, compost had the lowest moisture content at 14.1%, providing structural stability within the biocell and helping prevent excessive acid accumulation, thereby supporting stable methane generation. Centrifuged WWTP biosolids generally contain 72%–78% moisture (EPA 2000), aligning closely with the 75.4% measured in this study. The total volatile solids (VS) content further indicates the proportion of degradable organic matter present in each substrate. The VS values are 85.4%, 82.5%, and 80.6% for WWTP biosolids, compost, and green waste, respectively, indicating their high organic load. WWTP biosolids contain 1.8% total nitrogen (N) and 1.3% total phosphorus (P), providing essential nutrients for microbial growth but also posing a risk of ammonia accumulation, which may inhibit methanogenesis. These values are consistent with the typical concentrations of organic matter and nutrients found in biosolids. For example, Yang et al. (2023) reported biosolids from Jiujiang City containing 38.5% organic matter, 3.4% nitrogen, and 1.1% phosphorus. In comparison, compost (0.2% N, 0.1% P) and green waste (0.8% N, 0.02% P) are more carbon-rich but significantly lower in nutrient content. The higher nitrogen and phosphorus levels in biosolids help compensate for this nutrient deficiency, making them a more balanced substrate for anaerobic processes.

Baseline nutrient and contaminant levels in biosolids, compost, and green waste are presented in Table 3.

The macroelements in the Ambato WWTP biosolids, such as calcium (4.57 ± 0.32%), magnesium (4.86 ± 0.15%), and potassium (0.77 ± 0.06%), fall within expected ranges for biosolids used as soil amendments (Onchoke & Fateru 2021). The sulfate concentration (0.52 ± 0.11%) is relatively moderate, which suggests a potential buffering effect but also raises concerns about sulfate-associated metal mobilization. The presence of heavy metals in biosolids is a major concern. In the Ambato WWTP biosolids, aluminum (759.43 ± 7.52 $mg.kg^{-1}$), chromium (1166 ± 26 $mg.kg^{-1}$), and zinc (2683 ± 91 $mg.kg^{-1}$) are significantly high compared to the findings of literature (Martínez Durán et al. 2023, Onchoke & Fateru 2021). Arsenic (5.58 ± 1.37 $mg.kg^{-1}$)

Table 2: Physicochemical properties of three organic substrates-WWTP biosolids, compost, and green waste—utilized within the biocell system.

	pH	% Humidity wet basis	% Volatile solids	% Total N dry basis	% Total P dry basis
WWTP Biosolids	7.7 ± 0.1	75.4 ± 0.2	85.4 ± 0.1	1.8 ± 0	1.3 ± 0
Compost	8.6 ± 0.5	14.1 ± 0.1	82.5 ± 0	0.2 ± 0	0.1 ± 0
Green waste	7.2 ± 0.1	89.6 ± 0.3	80.6 ± 0.1	0.8 ± 0.1	0.02 ± 0

Table 3: Composition of Ambato WWTP Biosolids.

Component	WWTP Biosolids
Potassium (K□O) [%]	0.77 ± 0.06
Calcium (CaO) [%]	4.57 ± 0.32
Magnesium (MgO) v	4.86 ± 0.15
Sulfate [%]	0.52 ± 0.11
Copper [%]	0.002 ± 0.0
Iron [%]	0.26 ± 0.04
Manganese [%]	0.10 ± 0.01
Molybdenum [%]	0.0 ± 0.0
Zinc [%]	0.53 ± 0.02
Aluminum [mg.kg^{-1}]	759.43 ± 7.52
Arsenic [mg.kg^{-1}]	5.58 ± 1.37
Cadmium [mg.kg^{-1}]	0.88 ± 0.10
Chromium [mg.kg^{-1}]	1166 ± 25
Cobalt [mg.kg^{-1}]	65.75 ± 1.65
Copper [mg.kg^{-1}]	171.44 ± 5.04
Nickel [mg.kg^{-1}]	42.75 ± 0.18
Lead [mg.kg^{-1}]	21.69 ± 2.19
Zinc [mg.kg^{-1}]	2683 ± 91

and lead (21.69 ± 2.19 mg.kg^{-1}) remain below hazardous levels but should be continuously monitored due to their potential bioaccumulation. The relatively high zinc content suggests that these biosolids could serve as a micronutrient supplement for crops, as zinc is essential for plant enzyme functions (Saleem et al. 2022).

Biocell Operation

Leachate recirculation in biocells sustains methane production and influences microbial activity and system stability. However, moisture retention capacity may decline over time due to physical and biological transformations within the system, potentially leading to uneven waste biodegradation, decreased methane yield, and reduced overall efficiency.

The results of the statistical analyses indicate that all physicochemical and biological parameters measured in the biocells over the 12-week operational period exhibited statistically significant temporal variation, as determined by repeated measures ANOVA ($p < 0.0001$). This consistent trend across variables-including methane generation, pH, COD, sulfates, phosphates, ammonium, sulfide gas, iron, magnesium, Cr(VI), total chromium, and cadmium-underscores the dynamic metabolic and geochemical processes occurring within each biocell over time. Furthermore, one-way ANOVA revealed statistically significant differences among biocells for ammonium, leachate sulfide, iron, magnesium, total chromium, and cadmium, indicating that these variables are particularly sensitive to inter-biocell variability. In contrast, parameters such as methane generation, pH, COD, sulfates, phosphates, sulfide gas, and Cr(VI) did not exhibit statistically significant differences among biocells during the operational period. These findings may be attributed to the inherent heterogeneity of the materials used in each biocell, which can differentially influence the progression of microbial activity and physicochemical transformations across systems (Kjeldsen et al. 2002). To better understand these trends, the following section presents and discusses in detail the temporal evolution of each measured parameter throughout the 12-week operational period.

The leachate pH variation in the three biocells, shown in Fig. 3, reflects distinct microbial activity and waste degradation patterns. Initially, the pH ranged from 8.0 to 8.2, however, in the following weeks, it exhibited an increasing trend. Oscillations occurred throughout the weeks, with peaks and dips, reaching values between 8.4 and 8.6 by week 12, suggesting a dynamic system with a tendency toward alkaline conditions.

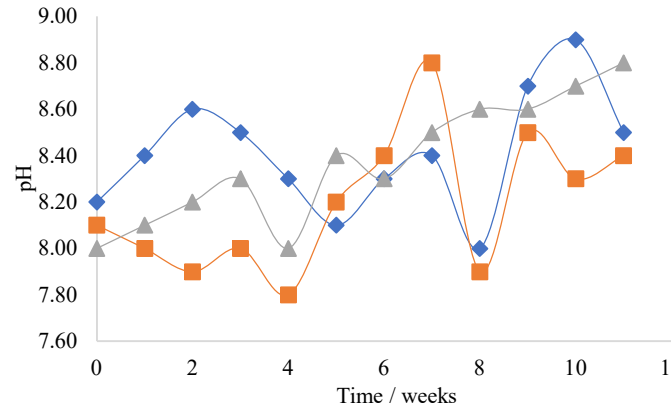

Fig. 3: pH monitoring from each biocell: (blue diamond) biocell 1; (orange square) biocell 2; and (gray triangle) biocell 3.

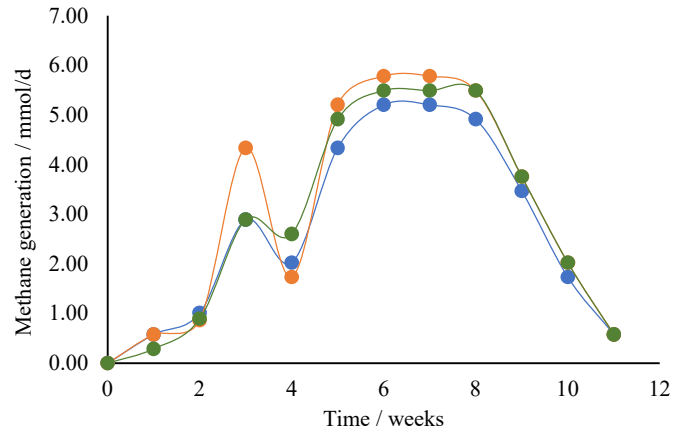

Fig. 4: Quantified methane gas from each biocell, (blue dot) biocell 1; (orange dot) biocell 2; and (green dot) biocell 3.

The pH range of 7.8 to 8.8 observed in the biocells aligns with conditions favorable for anaerobic and facultative microbial activities. While methanogenic bacteria typically thrive in a pH range of 6.6 to 7.6, other anaerobic microorganisms can function effectively in more alkaline environments. For instance, some anaerobic bacteria have been found to grow at pH levels up to 8.8, indicating that the pH conditions in the biocells are conducive to the activity of a diverse microbial community involved in organic matter degradation (Gerardi 2003).

Fig. 4 shows the quantified methane generation from each laboratory-scale biocell, measured at an average atmospheric pressure of 0.7 atm and a laboratory temperature of 22 °C. The data follow a characteristic curve with an initial phase of increasing biogas production, a steady methane generation phase between weeks 5 and 8, and a declining phase from weeks 8 to 12. The initial phase (0-1 week) of methane production in all three biocells exhibits a lag period characterized by low CH_4 volumes.

This lag period suggests that microbial communities are in an acclimatization phase, where hydrolytic and fermentative bacteria begin breaking down complex organic matter into simpler intermediates such as sugars, amino acids, and volatile fatty acids (VFAs) (Schievano et al. 2018). The delay in methane production indicates that methanogenic archaea have not yet reached full activity, as they rely on the byproducts of acidogenesis and acetogenesis, primarily acetate and hydrogen (H_2). At this stage, the similar methane production patterns among the three biocells suggest that their initial microbial inoculum or substrate composition did not differ significantly.

As described by He et al. (2019), the rapid rise in methane production observed around week 2-particularly in biocell 1-corresponds with established patterns of Methanosarcina barkeri activity and acetoclastic methanogenesis. Their findings indicate that Methanosarcina species perform efficiently under elevated acetate concentrations, which supports the early methane peaks recorded in this study. The delayed response in biocell 2 suggests a slower microbial adaptation, as the research indicates that acetate stress can hinder quorum sensing and slow methanogenesis. The lower peak in biocell 3 reflects a more balanced microbial adaptation, consistent with *Methanosarcina's* ability to shift pathways based on environmental stressors.

Following this peak, methane production experiences a noticeable decline between weeks 2.5 and 4 across all biocells. This temporary drop in biogas production can be attributed to several factors. One possible explanation is the depletion of readily biodegradable substrates, leading to a period where more complex compounds require enzymatic hydrolysis before being converted into methane precursors. Another likely cause is the accumulation of VFAs, which, if produced faster than methanogens can consume, can lead to a pH drop and partial inhibition of methanogenic activity. A microbial shift may occur, where acetoclastic methanogens are replaced or supplemented by hydrogenotrophic methanogens that utilize CO_2 and H_2 for methane production. This transition can introduce a temporary imbalance in the anaerobic digestion process, leading to fluctuations in CH_4 output (Hettiaratchi et al. 2015, Latif 2021).

The bioreactor landfill study at Sudokwon (Choi & Rhee 2024), the biocell methane production trends, and the metagenomic analysis of microbial methane cycling in landfills emphasize key factors influencing methane generation, microbial adaptation, and substrate utilization. In the Sudokwon study, leachate recirculation increased moisture content (38-39%), resulting in continuous landfill gas (LFG) production, whereas the reference zone (3D) with lower moisture (~26–29%) showed minimal LFG generation. This pattern is reflected in the biocell experiment, where

from weeks 4 to 9, methane production stabilized at 5.5 mmoL $CH_4.d^{-1}$, indicating that hydrolysis, acidogenesis, acetogenesis, and methanogenesis had reached equilibrium. The metagenomic landfill study further supports this by demonstrating that methanogenic microbial communities are more abundant and metabolically versatile in newer waste, leading to rapid methane production early in landfill life cycles. In comparison, older waste enters a phase of slower methanogenesis due to substrate depletion. The Sudokwon landfill study also found that the cellulose-to-lignin ($Ce.L^{-1}$) ratio exhibited a significantly higher reaction rate than the C/N ratio, indicating that cellulose decomposes more rapidly than nitrogen-based compounds. This corresponds to the period between weeks 9 and 11 in the biocell experiment, during which methane production declines as the readily degradable organic matter becomes depleted, leaving behind more recalcitrant components such as lignin.

Additionally, the delayed methane production in biocell 2 aligns with the reference zone (3D) in the Sudokwon landfill, where lower moisture slowed microbial adaptation and waste degradation. The metagenomic analysis of landfill methanogens indicates that oxygen-limited conditions and substrate availability shape microbial community succession, influencing methane yield over time. The decline in methane production observed in weeks 9-11 of the biocell study could be due to substrate depletion, microbial aging, and inhibitory byproducts such as NH_4^+, a trend also noted in the landfill study, where older waste exhibited reduced methanogenic activity and increased potential for methane oxidation (Grégoire et al. 2023).

Comparing the three biocells, biocell 1 demonstrated the fastest initial methane production but also exhibited a more pronounced decline post-peak, suggesting a system optimized for rapid substrate utilization but with limited long-term stability. In contrast, biocell 2 had a delayed peak but achieved methane levels comparable to the other biocells in the steady-state phase, indicating a possible higher proportion of complex organic matter in its substrate. Biocell 3, which showed a more gradual and balanced response throughout, appears to have the most stable performance, potentially due to a well-maintained microbial equilibrium or better buffering capacity within the system.

The Chemical Oxygen Demand (COD) profile in Fig. 5, biocell 1, biocell 2, and biocell 3, provides crucial insights into the organic matter degradation process and its correlation with pH fluctuations and methane (CH_4) production. COD represents the concentration of biodegradable and non-biodegradable organic matter, and its variation over time reflects the efficiency of microbial activity in anaerobic digestion.

The COD decline from weeks 0-2, particularly the sharp drop in biocell 2 (~1300 ppm to ~800 ppm), suggests rapid degradation of easily hydrolyzable organic matter, which is consistent with the high organic load degradation observed in food waste anaerobic digestion (FW-AD) (Perin et al. 2020). This degradation aligns with the early pH drop observed in biocell 2, where an accumulation of volatile fatty acids (VFAs) likely occurred. In contrast, biocell 1 and biocell 3 show a more gradual COD reduction, suggesting a slower but more controlled hydrolysis process. The previously analyzed methane production data indicated that biocell 1 exhibited the highest initial CH_4 peak, which corresponds to a moderate COD decrease, confirming that methanogenesis efficiently converted intermediates into methane (Dang et al. 2023). However, in biocell 2, the lower initial methane yield and unstable pH suggest that excessive VFAs may

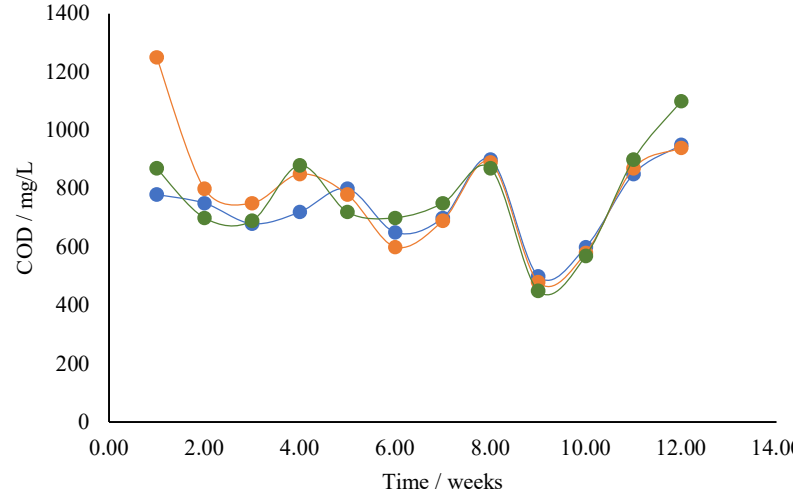

Fig. 5: Weekly COD monitoring: (blue dot) biocell 1; (orange dot) biocell 2; and (green dot) biocell 3.

have temporarily inhibited methanogenesis, leading to higher residual COD concentrations in the subsequent weeks.

Between weeks 2 and 8, all three biocells exhibit COD fluctuations, which align with pH oscillations and methane production variations. These fluctuations suggest intermittent substrate hydrolysis and VFA accumulation phases, followed by methanogenic activity consuming these intermediates. Around weeks 6-8, a COD decline is observed, corresponding to stable methane production and increasing pH in biocell 1 and biocell 3, indicating efficient organic matter conversion. In contrast, biocell 2 exhibits (Zhang et al. 2011) more erratic COD values, correlating with its observed pH drops and methane dips, suggesting ongoing acidification stress. Finally, from weeks 8-12, all

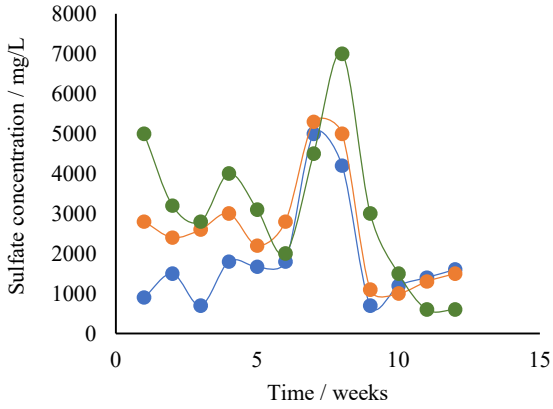

a

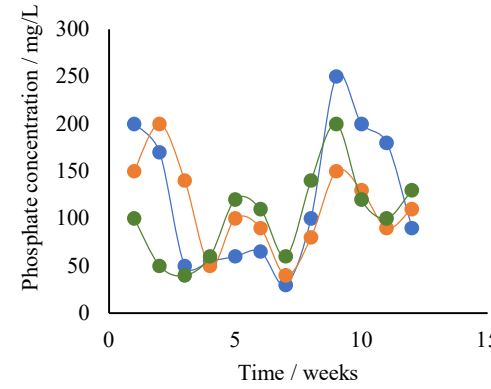

b

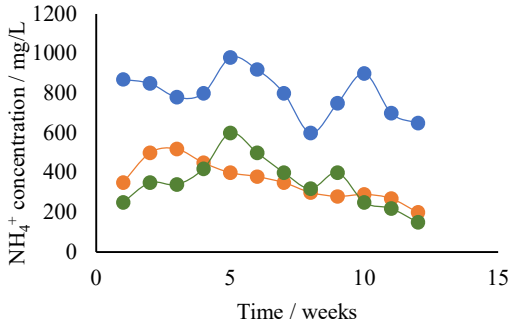

C

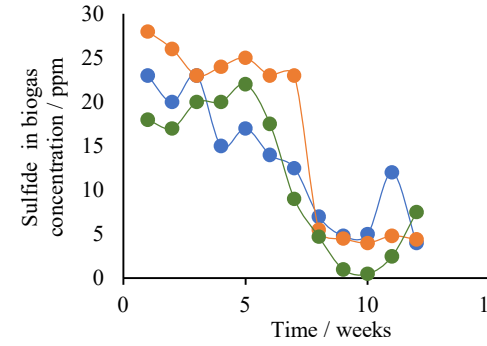

d

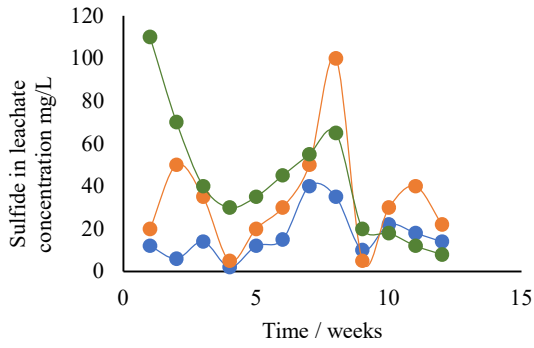

e

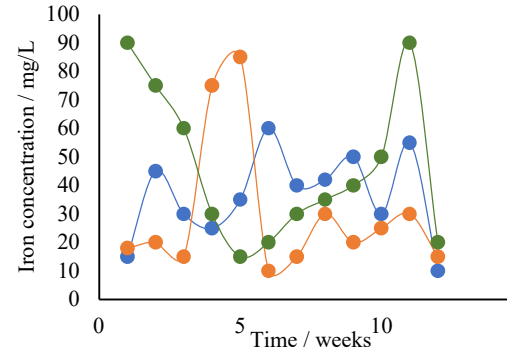

f

Figure Cont....

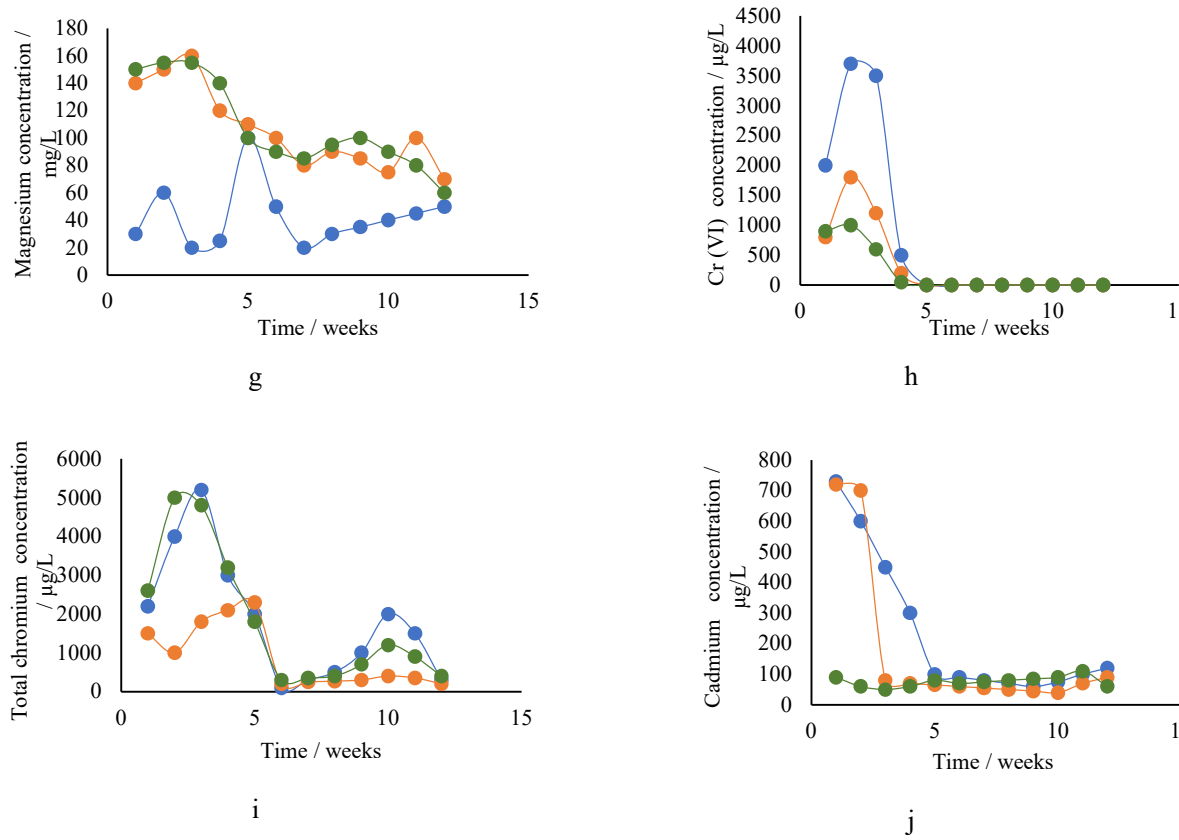

Fig. 6: Weekly Monitoring of Inorganic Compounds and Heavy Metals in Biocells: a) sulfate, b) phosphate monitoring, c) ammonium, d) sulfide in biogas, e) sulfide in leachate, f) iron, g) magnesium, h) chromium VI, i) total chromium, j) cadmium where (blue dot) biocell 1; (orange dot) biocell 2; and (green dot) biocell 3.

biocells experienced a COD increase, likely due to substrate depletion and reduced microbial activity. This final COD rise corresponds to the late-stage pH increase in biocell 1 and the decline in methane production, reinforcing the hypothesis that microbial activity is slowing at this stage, and residual recalcitrant organic matter remains unprocessed. These results show that stable pH regulation is crucial for efficient COD removal and sustained methane generation.

In Fig. 6a, sulfate concentrations show substantial fluctuations across all biocells. Biocell 2 starts with a high sulfate concentration (~5000 $mg.L^{-1}$) and rapidly declines, while biocell 1 and biocell 3 show a more gradual reduction after week 3. This trend suggests active sulfate-reducing bacteria (SRB) (Xia et al. 2014), which convert SO_4^{2-} into hydrogen sulfide (H_2S) under anaerobic conditions. The sharp drop in biocell 2 may indicate intense sulfate reduction activity, potentially linked to VFA accumulation and pH drops observed previously. The slower sulfate consumption in biocell 1 and biocell 3 suggests a more controlled microbial response, potentially reducing the risk of H_2S toxicity to methanogens (Jin et al. 2020, Ying et al. 2019).

The study on iron oxide-biochar composites by Wu et al. (2020) provides insight into the phosphate stability observed in the biocell landfill simulation. In Fig. 6b, phosphate concentrations remain stable (40–250 $mg.L^{-1}$), suggesting a balance between microbial uptake, solubilization, and potential adsorption onto mineral surfaces. The increase in phosphate levels in weeks 8–12 likely results from cell lysis and microbial turnover, releasing phosphorus into the system. The variability in biocell 2 may be linked to acidification effects on phosphate solubility, similar to Fe(III) biochar findings, which remain stable under pH fluctuations. The biochar study's 86.4% reduction in phosphate leaching suggests that iron-phosphate interactions could play a role in nutrient retention within the biocells, minimizing phosphorus loss into leachate. Iron-mediated adsorption and microbial cycling likely regulate phosphorus availability in the biocells, contributing to long-term stability and reduced leaching potential.

Fig. 6c, ammonium levels start high (~800-1000 $mg.L^{-1}$) and decline steadily in all biocells. This decreasing trend suggests effective ammonium uptake by

microbial communities or volatilization under alkaline conditions. Biocell 2 has the highest initial ammonium concentration (~1000 $mg.L^{-1}$), but its reduction rate is slower than biocell 1 and biocell 3, indicating a delayed microbial adaptation in biocell 2 or VFA accumulation inhibiting nitrification processes. By week 10, ammonium levels in biocell 1 and biocell 3 stabilize at ~250 $mg.L^{-1}$, which coincides with reduced methane production, suggesting substrate exhaustion and declining microbial activity (González-Cortés et al. 2021).

Fig. 6d and 6e, the higher sulfide concentrations in biogas compared to leachate in early weeks suggest that sulfate reduction was more active in the gas phase initially, whereas in leachate, sulfate-to-sulfide conversion varied depending on cell conditions. The delayed sulfide peak in biocell 2's leachate (week 8) corresponds with its relatively stable sulfide levels in biogas, suggesting that sulfate was retained in solution longer before microbial reduction became dominant. Biocell 3 exhibited the highest initial sulfide accumulation in leachate, which declined steadily, whereas biocell 1 demonstrated more stable sulfide trends in biogas and leachate. These differences indicate variable sulfate reduction rates, substrate availability, and microbial adaptation between biocells, affecting the balance between sulfide retention in the liquid phase and release as hydrogen sulfide in biogas (Long et al. 2016).

Fig. 6f, iron concentrations fluctuate across all biocells, with a steady decline from ~100 $mg.L^{-1}$ to ~20 $mg.L^{-1}$ by week 10, suggesting that iron is being consumed by iron-reducing bacteria (IRB) or precipitated as FeS due to sulfide interactions. Biocell 1 and biocell 3 show a more rapid iron decrease, suggesting stronger iron-dependent microbial activity, potentially enhancing redox reactions that influence electron flow in anaerobic digestion. Biocell 2 maintains residual Fe levels, possibly helping to buffer against excessive sulfide accumulation.

Fig. 6g, magnesium concentrations remain relatively stable in all biocells but drop slightly after week 6 (~90 to ~50 $mg.L^{-1}$). This decline suggests incorporation into microbial biomass (Liu et al. 2019) or precipitation as $MgNH_4PO_4$ (struvite), a common byproduct in anaerobic digestion (Muhmood et al. 2019). Stabilization in biocell 3 aligns with more controlled pH trends, reinforcing the importance of alkalinity in preventing nutrient losses.

Fig. 6h and 6i, comparing total chromium (Cr-total) and hexavalent chromium (Cr-VI) concentrations across the biocells, reveal distinct reduction trends and transformation dynamics during the experimental period. Initially, Cr-total concentrations in all biocells are high, with peaks occurring at week 3 (biocell 1: 5200 $\mu g.L^{-1}$, biocell 2: 1800 $\mu g.L^{-1}$, biocell 3: 4800 $\mu g.L^{-1}$), indicating significant chromium mobilization, likely from the degradation of organic matter or dissolution of metal complexes. Over time, Cr-total concentrations decrease substantially, reaching below 500 $\mu g.L^{-1}$ in all biocells by week 12, suggesting progressive chromium precipitation or microbial-mediated immobilization. In contrast, Cr-VI shows a sharp decline much earlier, reaching undetectable levels by week 5, with initial peaks in biocell 1 (3700 $\mu g.L^{-1}$ at week 2), biocell 2 (1800 $\mu g.L^{-1}$ at week 2), and biocell 3 (1000 $\mu g.L^{-1}$ at week 2), followed by rapid depletion by week 4 due to an effective reduction process, likely driven by anaerobic microbial activity facilitating electron transfer and Cr-VI reduction to the less toxic Cr-III form. Cr-total persistence beyond week 5 suggests that a portion remains in less bioavailable fractions, possibly as precipitates (e.g., chromium hydroxides) or bound within organic matrices. The faster reduction of Cr-VI compared to Cr-total suggests that biogeochemical conditions within the biocells favor detoxification mechanisms, potentially involving sulfate-reducing bacteria (SRB) (Yang et al. 2021) or iron-mediated reduction pathways, which are known to facilitate Cr-VI to Cr-III conversion in anaerobic environments.

In Fig. 6j, cadmium concentrations exhibit a progressive decline from ~120 $\mu g.L^{-1}$ to ~50 $\mu g.L^{-1}$ across all biocells, indicating effective metal immobilization through adsorption onto biomass, precipitation, or complexation with sulfides. Biocell 3 demonstrates slightly lower Cd levels in later weeks, suggesting enhanced removal efficiency, potentially driven by a more diverse microbial community or stronger interactions with sulfide and iron species. This trend aligns with the findings of Zhang et al. 2023), who investigated landfill leachate sludge-derived biochar (LLSDB) and reported that low Cd concentrations follow a linear adsorption model (physical adsorption). In contrast, higher concentrations engage in chemical adsorption mechanisms. The observed cadmium reduction in the biocells suggests a transition from initial physical adsorption onto organic matrices to subsequent chemical stabilization via sulfide precipitation or complexation with iron oxides, reinforcing the role of microbial and geochemical processes in heavy metal remediation.

The characterization of the solid phase at the end of biogas production, Table 4, provides crucial insights into the retention, transformation, and environmental behavior of key inorganic compounds, including sulfates, phosphates, magnesium, chromium, and cadmium (Frank et al. 2017). Sulfate concentrations were highest in biosolids (156.1 $g.kg^{-1}$ in biocell 1), indicating significant retention. At the same time, lower levels in compost and plant matter suggest partial sulfate reduction via sulfate-reducing bacteria (SRB)

Table 4: The concentration of key inorganic compounds (sulfates, phosphates, magnesium, chromium VI, total chromium, and cadmium) in the solid phase (biosolids, compost, and green waste) of the three biocells at the end of biogas production.

Compound	Biocell	WWTP Biosolids	Compost	Green waste
	1	156.1 ± 4.71	74.02 ± 0	54.1 ± 0
Sulfate, $mg.kg^{-1}$	2	112.3 ± 4.71	69.6 ± 5.18	30.7 ± 0
	3	115.9 ± 5.77	90.6 ± 5.77	26.2 ± 0
	1	8.8 ± 0.94	8.9 ± 1.41	3.7 ± 0.81
Phosphate, $mg.kg^{-1}$	2	6.7 ± 0.47	6.04 ± 0.94	0.7 ± 0.47
	3	8.2 ± 0.78	6.1 ± 0.31	0.9 ± 1.24
	1	4.5 ± 0.8	2.3 ± 0.4	0.8 ± 0
Magnesium, $mg.kg^{-1}$	2	4.4 ± 0.7	1.7 ± 0.8	1.2 ± 0.3
	3	4.5 ± 0.7	1.7 ± 0.3	0.7 ± 0.1
	1	1.4 ± 0.7	1.1 ± 0.3	0.6 ± 0.7
Total Chromium, $mg.kg^{-1}$	2	1.2 ± 0.5	0.9 ± 0.1	0.5 ± 0.1
	3	1.5 ± 0.5	1.1 ± 0.2	0.7 ± 0.1
	1	0.10 ± 0.06	0.08 ± 0.03	0.06 ± 0001
Cadmium, $mg.kg^{-1}$	2	0.10 ± 0,07	0.07 ± 0.04	0.06 ± 0.09
	3	0.10 ± 0.08	0.07 ± 0.06	0.07 ± 0.02

(Ghosh et al. 2020). Phosphates remained stable in biosolids and compost but were significantly lower in green waste, demonstrating that phosphorus is primarily retained within the solid matrix. Magnesium exhibited a progressive decline from biosolids to compost to green waste, likely due to mineral precipitation as struvite ($MgNH_4PO_4 \cdot 6H_2O$).

Total chromium and cadmium concentrations were low across all biocells, but trace cadmium was detected in plant residues (~0.06–0.07 $mg.kg^{-1}$), suggesting a potential bioaccumulation risk. Comparatively, biocell 3 exhibited the highest retention of sulfate, phosphate, magnesium, and chromium, indicating greater stabilization efficiency. These findings emphasize the need for optimized redox control, sulfate management to limit excess sulfide formation, and enhanced phosphorus recovery strategies, while cadmium retention in plant biomass warrants further investigation into its environmental risks and mitigation strategies.

CONCLUSIONS

This study demonstrates the crucial role of biocell design and operational parameters in optimizing anaerobic waste degradation and biogas production. The strategic integration of WWTP biosolids, compost, and green waste promoted a balanced microbial ecosystem, facilitating efficient methanogenesis and organic matter stabilization. The results confirm that a well-structured layering system and controlled leachate recirculation and moisture management enhance substrate bioavailability, directly impacting methane yields and leachate composition. The variability in methane production across biocells highlights the influence of waste composition, microbial adaptation, and nutrient availability in determining bioreactor performance.

Methane generation followed a characteristic pattern, with biocell 1 achieving rapid initial methane production but experiencing early substrate depletion and unstable long-term performance. In contrast, biocell 2 exhibited a delayed but sustained methane peak, indicative of the gradual breakdown of complex organic matter and a slower microbial adaptation process. Biocell 3 demonstrated the most stable methane output, suggesting that its composition and buffering capacity supported microbial equilibrium over time. The decline in methane production after week nine across all biocells suggests substrate depletion and potential microbial inhibition due to ammonia accumulation, reinforcing the need for optimized nutrient ratios to sustain methanogenesis.

Leachate recirculation was vital in sustaining methane production, influencing microbial activity, and affecting system longevity. The high initial leachate retention (~65%) facilitated methanogenic bacterial proliferation, but retention capacity declined significantly after week two (~11-13%), highlighting changes in system permeability and moisture absorption. These findings emphasize the necessity for adaptive leachate management strategies to sustain high retention rates and prevent excessive leachate loss, which could lead to uneven waste degradation and reduced biogas yields. The pH dynamics in the biocells further underscored the complexity of microbial interactions, with biocell 3 exhibiting the most stable pH profile, supporting

consistent methanogenesis, while biocell 1 and biocell 2 experienced fluctuations corresponding to microbial stress and acidification.

Nutrient cycling and heavy metal immobilization were also significantly influenced by biocell conditions. WWTP biosolids were crucial in supplying essential nutrients such as nitrogen, phosphorus, and potassium, enhancing microbial metabolic activity. Chromium (VI) was effectively reduced to the less toxic Cr(III), confirming that microbial-mediated detoxification processes were active within the biocells. Additionally, cadmium bioavailability decreased over time, suggesting successful immobilization through sulfide precipitation and iron oxide complexation. The differences in heavy metal retention between biocells indicate that optimizing redox conditions and microbial community composition could further enhance metal stabilization.

Several optimization strategies should be considered to improve biocell performance. Organic substrate composition should be adjusted to balance the C/N ratio and sustain microbial activity and methane production. Moisture management and leachate recirculation must be dynamically adjusted based on real-time microbial activity and substrate degradation monitoring to prevent excessive leachate loss and maintain optimal moisture levels. Furthermore, enhancing microbial consortia through bioaugmentation strategies could improve both methane yields and heavy metal immobilization, making biocell technology a more effective tool for landfill waste stabilization.

In summary, this study assesses the viability of biocell technology as a sustainable waste management alternative for Ambato, highlighting its potential to improve waste stabilization and reduce environmental impact. The results underscore the need for optimizing operational parameters, microbial dynamics, and nutrient balance to maintain efficient methanogenesis and effective leachate management. Successful implementation could enhance methane recovery as a renewable energy source while limiting heavy metal mobility and ensuring long-term environmental stability.

Future research should focus on developing adaptive biocell designs that integrate bioaugmentation with specialized microbial consortia and enzymatic catalysts to enhance organic matter degradation, optimize methane production, prevent contaminant migration, and strengthen the overall environmental sustainability of waste management systems. Additionally, since the biocells were evaluated under laboratory-scale conditions, pilot-scale field studies are necessary to address the operational and environmental complexities of real landfill settings. Such validation would also help assess long-term performance, scalability, and adaptability under diverse waste compositions and climatic conditions. Addressing these aspects in future research will facilitate the transition from laboratory-scale experimentation to practical, full-scale implementation.

ACKNOWLEDGMENTS

This research was funded by the Ecuadorian Corporation for Research and Academia Development (CEDIA) through the IDi Fund Universities, IDi XVIII 2023, as part of Project I+D+I-XVIII-2023-50: "Development of a Toxicological Testing Platform in Zebrafish (Danio rerio) for the Discovery of New Environmental Contaminants and the Evaluation of Water Quality to Assess the Effectiveness of Decontamination Treatments."

We gratefully acknowledge the support of the Research and Development Directorate (DIDE), the Faculty of Food Science and Biotechnology Engineering (FCIAB), and the Technical University of Ambato (UTA), Ecuador. Special thanks are extended to the Ambato Municipal Water and Sanitation Company (EP-EMAPA-A) and the Wastewater Treatment Plant (WWTP) for their valuable collaboration and provision of biosolids samples.

We also recognize the contributions of the research groups Gestión de Recursos Naturales e Infraestructura Sustentable (GeReNIS) and G+ Bio-Food and Engineering of UTA, whose insights enriched this work. Additional appreciation is given to the Project Canje de Deuda Ecuador–España: Fortalecimiento de la unidad operativa de investigación (FITA-UOITA) for their collaboration.

Finally, we thank UTA and DIDE for their institutional backing, resources, coordination, and technical assistance, which were instrumental to the successful execution of this study.

REFERENCES

Aldrawsha, A., Natarajan, R. and Ibrahim, O., 2020. Biogas production from waste in a sanitary landfill reactor. *Journal of Thermal Engineering*, 6(6), pp.298–311. [DOI]

American Public Health Association (APHA), 2017. *Standard Methods for the Examination of Water and Wastewater* (23rd ed.). American Public Health Association.

Budihardjo, M.A., Ramadan, B.S., Yohana, E., Syafrudin, Rahmawati, F., Ardiana, R., Susilo, D.B., Ikhlas, N. and Karmilia, A., 2021. A review of anaerobic landfill bioreactor using leachate recirculation to increase methane gas recovery. *IOP Conference Series: Earth and Environmental Science*, 894(1). [DOI]

Chen, D.M.C., Bodirsky, B.L., Krueger, T., Mishra, A. and Popp, A., 2020. The world's growing municipal solid waste: Trends and impacts. *Environmental Research Letters*, 15(7). [DOI]

Choi, H.-J. and Rhee, S.-W., 2024. The effect of waste degradation on landfill gas production in field-scale bioreactor landfill. *Journal of Material Cycles and Waste Management*, 26(1), pp.400–409. [DOI]

Dang, Q., Zhao, X., Li, Y. and Xi, B., 2023. Revisiting the biological pathway for methanogenesis in landfill from metagenomic perspective: A case study of county-level sanitary landfill of domestic waste in North China Plain. *Environmental Research*, 222, p.115185. [DOI]

Environmental Protection Agency (EPA), 2000. *Biosolids Technology Fact Sheet: Centrifuge Thickening and Dewatering*. U.S. Environmental Protection Agency. Retrieved from https://www3.epa.gov/npdes/pubs/centrifuge_thickening.pdf

Environmental Protection Agency (EPA), 2007. *Method 3051A: Microwave Assisted Acid Digestion of Sediments, Sludges, and Oils*. U.S. Environmental Protection Agency. Retrieved from https://www.epa.gov/sites/default/files/2015-12/documents/3051a.pdf

Environmental Protection Agency (EPA), 2024. *Inventory of U.S. Greenhouse Gas Emissions and Sinks: 1990–2022 – Main Text*. U.S. Environmental Protection Agency. Retrieved from https://nepis.epa.gov/Exe/ZyPDF.cgi/901U0S00.PDF?Dockey=901U0S00.PDF

Essien, J.P., Ikpe, D.I., Inam, E.D., Okon, A.O., Ebong, G.A. and Benson, N.U., 2022. Occurrence and spatial distribution of heavy metals in landfill leachates and impacted freshwater ecosystem: An environmental and human health threat. *PLoS ONE*, 17(2). [DOI]

Frank, R.R., Cipullo, S., Garcia, J., Davies, S., Wagland, S.T., Villa, R., Trois, C. and Coulon, F., 2017. Compositional and physicochemical changes in waste materials and biogas production across seven landfill sites in the UK. *Waste Management*, 63, pp.11–17. [DOI]

GAD Municipal de Ambato, 2016. *Ambato: An Example of Sustainability in the Region*. Retrieved from https://gadmatic.ambato.gob.ec/lotaip/2016/octubre/anexo%20literal%20m/Boletines/Ambato%20ejemplo%20de%20sostenibilidad%20en%20la%20regio%CC%81n.pdf

Gerardi, M., 2003. *The Microbiology of Anaerobic Digesters*. John Wiley & Sons, Inc.

Ghosh, P., Kumar, M., Kapoor, R., Kumar, S.S., Singh, L., Vijay, V., Vijay, V.K., Kumar, V. and Thakur, I.S., 2020. Enhanced biogas production from municipal solid waste via co-digestion with sewage sludge and metabolic pathway analysis. *Bioresource Technology*, 296, p.122275. [DOI]

González-Cortés, J.J., Almenglo, F., Ramírez, M. and Cantero, D., 2021. Simultaneous removal of ammonium from landfill leachate and hydrogen sulfide from biogas using a novel two-stage oxic–anoxic system. *Science of the Total Environment*, 750, p.141664. [DOI]

Grégoire, D.S., George, N.A. and Hug, L.A., 2023. Microbial methane cycling in a landfill on a decadal time scale. *Nature Communications*, 14(1). [DOI]

Hadi, N.S., 2023. Leachate characterization and assessment of soil pollution near municipal solid waste transfer stations in Baghdad City. *Nature Environment and Pollution Technology*, 22(4), pp.2239–2247. [DOI]

He, P., Duan, H., Han, W., Liu, Y., Shao, L. and Lü, F., 2019. Responses of *Methanosarcina barkeri* to acetate stress. *Biotechnology for Biofuels*, 12(1), p.289. [DOI]

Hettiaratchi, P., Jayasinghe, P., Tay, J. and Yadav, S., 2015. Recent advances of biomass waste to gas using landfill bioreactor technology: A review. *Current Organic Chemistry*, 19(5), pp.413–422. [DOI]

Hussein, M., Yoneda, K., Mohd-Zaki, Z., Amir, A. and Othman, N., 2021. Heavy metals in leachate, impacted soils and natural soils of different landfills in Malaysia: An alarming threat. *Chemosphere*, 267. [DOI]

Instituto Nacional de Estadística y Censos (INEC), 2023. 2022 National Census Results: Population Density by Canton. Retrieved from https://www.censoecuador.gob.ec/wp-content/uploads/2023/10/2022_CPV_NACIONAL_DENSIDAD_POBLACIONAL.xlsx

Intergovernmental Panel on Climate Change (IPCC), 2023. Sixth Assessment Report: Climate Change 2023. [DOI]

Japperi, N.S., Mohd Asri, Z.Z., Wan Bakar, W.Z., Dollah, A., Ahmad Fuad, M.F.I. and Che Mohamed Hussein, S.N., 2021. Review on landfill gas formation from leachate biodegradation. *Malaysian Journal of Chemical Engineering and Technology*, 4(1). [DOI]

Jin, Z., Ci, M., Yang, W., Shen, D., Hu, L., Fang, C. and Long, Y., 2020. Sulfate reduction behaviour in the leachate-saturated zone of landfill sites. *Science of the Total Environment*, 730, p.138946. [DOI]

Kjeldsen, P., Barlaz, M.A., Rooker, A.P., Baun, A., Ledin, A. and Christensen, T.H., 2002. Present and long-term composition of MSW landfill leachate: A review. *Critical Reviews in Environmental Science and Technology*, 32(4), pp.297–336. [DOI]

Kumar, S., Mudhoo, A. and Chiemchaisri, C., 2011. Bioreactor landfill technology in municipal solid waste treatment: An overview. *Critical Reviews in Biotechnology*, 31(1), pp.77–97. [DOI]

Latif, M.B., 2021. *Effect of Sludge Content on Different Types of Food Waste Degradation in Anaerobic Digester*. University of Texas at Arlington. Retrieved from https://mavmatrix.uta.edu/civilengineering_theses/410

Liu, S., Xi, B.-D., Qiu, Z.-P., He, X.-S., Zhang, H., Dang, Q.-L., Zhao, X.-Y. and Li, D., 2019. Succession and diversity of microbial communities in landfills with depths and ages and their association with dissolved organic matter and heavy metals. *Science of the Total Environment*, 651, pp.909–916. [DOI]

Long, Y., Fang, Y., Shen, D., Feng, H. and Chen, T., 2016. Hydrogen sulfide (H_2S) emission control by aerobic sulfate reduction in landfill. *Scientific Reports*, 6, p.38103. [DOI]

Martínez Durán, A.J., Rodríguez Núñez, V.A. and Castillo Jáquez, J.C., 2023. Use of biosolids from wastewater treatment plants and other organic fertilizers in agriculture: Preliminary results of a case study in banana cultivation in the Dominican Republic. *Frontiers in Water*, 5. [DOI]

Mojiri, A., Zhou, J.L., Ratnaweera, H., Ohashi, A., Ozaki, N., Kindaichi, T. and Asakura, H., 2021. Treatment of landfill leachate with different techniques: An overview. *Journal of Water Reuse and Desalination*, 11(1), pp.66–96. [DOI]

Muhmood, A., Lu, J., Dong, R. and Wu, S., 2019. Formation of struvite from agricultural wastewaters and its reuse on farmlands: Status and hindrances to closing the nutrient loop. *Journal of Environmental Management*, 230, pp.1–13. [DOI]

Nopharatana, A., Clarke, W.P., Pullammanappallil, P.C., Silvey, P. and Chynoweth, D.P., 1998. Evaluation of methanogenic activities during anaerobic digestion of municipal solid waste. *Bioresource Technology*, 64, pp.169–174. [DOI]

Onchoke, K.K. and Fateru, O.O., 2021. Evaluating bioavailability of elements in municipal wastewater sludge (biosolids) from three rural wastewater treatment plants in East Texas (USA) by a sequential extraction procedure. *Results in Chemistry*, 3. [DOI]

Perin, J.K., Biesdorf Borth, P.L., Torrecilhas, A.R., Santana da Cunha, L., Kuroda, E.K. and Fernandes, F., 2020. Optimization of methane production parameters during anaerobic co-digestion of food waste and garden waste. *Journal of Cleaner Production*, 272, p.123130. [DOI]

Saleem, M., Usman, K., Rizwan, M., Al Jabri, H. and Alsafran, M., 2022. Functions and strategies for enhancing zinc availability in plants for sustainable agriculture. In: *Frontiers in Plant Science*, Vol.13. Frontiers Media S.A. [DOI]

Sanchez-Salvador, J.L., Marques, M.P., Brito, M.S.C.A., Negro, C., Monte, M.C., Manrique, Y.A., Santos, R.J. and Blanco, A., 2022. Valorization of vegetable waste from leek, lettuce, and artichoke to produce highly concentrated lignocellulose micro- and nanofibril suspensions. *Nanomaterials*, 12(24). [DOI]

Sanoop, G., Cyrus, S., and Madhu, G. 2024. Sustainability analysis of landfill cover system constructed using recycled waste materials by life cycle assessment. *Nature Environment and Pollution Technology*, 23(1), pp.409–417. [DOI]

Schievano, A., Colombo, A., Cossettini, A., Goglio, A., D'Ardes, V., Trasatti, S. and Cristiani, P., 2018. Single-chamber microbial fuel cells as on-line shock-sensors for volatile fatty acids in anaerobic digesters. *Waste Management*, 71, pp.785–791. [DOI]

Shao, Y., Xia, M., Liu, J., Liu, X. and Li, Z., 2021. Composition and

profiles of volatile organic compounds during waste decomposition by the anaerobic bacteria purified from landfill. *Waste Management*, 126, pp.466–475. [DOI]

Sorensen, A.H. and Ahring, B.K., 1993. Measurements of the specific methanogenic activity of anaerobic digestor biomass. *Applied Microbiology and Biotechnology*, 40, pp.427–431. [DOI]

Vaverková, M.D., 2019. Landfill impacts on the environment—review. In: *Geosciences (Switzerland)*, Vol.9, Issue 10. MDPI AG. [DOI]

Werkneh, A.A., 2022. Biogas impurities: Environmental and health implications, removal technologies and future perspectives. In: *Heliyon*, Vol.8, Issue 10. Elsevier Ltd. [DOI]

Wu, L., Zhang, S., Wang, J. and Ding, X., 2020. Phosphorus retention using iron (II/III) modified biochar in saline-alkaline soils: Adsorption, column and field tests. *Environmental Pollution*, 261, p.114223. [DOI]

Xia, F.F., Su, Y., Wei, X.M., He, Y.H., Wu, Z.C., Ghulam, A. and He, R., 2014. Diversity and activity of sulphur-oxidizing bacteria and sulphate-reducing bacteria in landfill cover soils. *Letters in Applied Microbiology*, 59(1), pp.26–34. [DOI]

Yang, Q., Zhao, Y., Wang, J., Zhou, H., Xiong, H., Zeng, M., Chen, L. and Huang, N., 2023. Components of sludge from municipal wastewater treatment plants and its evaluation for land application in JiUJiang city of China. In: *Advances in Engineering Technology Research ISEEMS*, 2023(8).

Yang, S., Li, L., Peng, X., Zhang, R. and Song, L., 2021. Methanogen community dynamics and methanogenic function response to solid waste decomposition. *Frontiers in Microbiology*, 12. [DOI]

Yang, Z., Liu, Z., Dabrowska, M., Debiec-Andrzejewska, K., Stasiuk, R., Yin, H. and Drewniak, L., 2021. Biostimulation of sulfate-reducing bacteria used for treatment of hydrometallurgical waste by secondary metabolites of urea decomposition by *Ochrobactrum* sp. POC9: From genome to microbiome analysis. *Chemosphere*, 282, p.131064. [DOI]

Ying, L., Long, Y., Yao, L., Liu, W., Hu, L., Fang, C. and Shen, D., 2019. Sulfate reduction at micro-aerobic solid–liquid interface in landfill. *Science of the Total Environment*, 667, pp.545–551. [DOI]

Zhang, C., Guo, Y., Wang, X. and Chen, S., 2019. Temporal and spatial variation of greenhouse gas emissions from a limited-controlled landfill site. *Environment International*, 127, pp.387–394. [DOI]

Zhang, H., Lu, K., Zhang, J., Ma, C., Wang, Z. and Tian, X., 2023. Removal and adsorption mechanisms of phosphorus, Cd and Pb from wastewater conferred by landfill leachate sludge-derived biochar. *Sustainability*, 15(13), p.10045. [DOI]

Zhang, L., Lee, Y.-W. and Jahng, D., 2011. Anaerobic co-digestion of food waste and piggery wastewater: Focusing on the role of trace elements. *Bioresource Technology*, 102(8), pp.5048–5059. [DOI]

Zhang, Z., Chen, Z., Zhang, J., Liu, Y., Chen, L., Yang, M., Osman, A.I., Farghali, M., Liu, E., Hassan, D., Ihara, I., Lu, K., Rooney, D.W. and Yap, P.S., 2024. Municipal solid waste management challenges in developing regions: A comprehensive review and future perspectives for Asia and Africa. *Science of the Total Environment*, 930. [DOI]